

Recent Results from SND@LHC

E. V. Khalikov^{1*} and E. D. Ursov^{2,1}

(on behalf of the SND@LHC Collaboration)

¹*Skobeltsyn Institute of Nuclear Physics, Lomonosov Moscow State University,
Moscow, Russia*

²*National University of Science and Technology “MISIS,” Moscow, Russia*

Received May 15, 2024; revised May 31, 2024; accepted June 1, 2024

Abstract—The Scattering and Neutrino Detector (SND@LHC) is a compact and stand-alone experiment to perform measurements with neutrinos produced at the LHC in a hitherto unexplored pseudorapidity region of $7.2 < \eta < 8.4$, complementary to all the other experiments at the LHC. The experiment is located 480 m downstream of IP1 in the unused TI18 tunnel. The detector is composed of a hybrid system based on an ~ 800 kg target mass of tungsten plates, interleaved with emulsion and electronic trackers, followed downstream by a calorimeter and a muon system. The configuration allows to efficiently distinguish between all three neutrino flavors, opening a unique opportunity to probe the physics of heavy flavor production at the LHC in the region that is not accessible to ATLAS, CMS, and LHCb. This region is of particular interest also for future circular colliders and for predictions of very high-energy atmospheric neutrinos. The physics program includes studies of charm production and lepton universality tests in the neutral sector. The detector concept is also well suited to searching for feebly interacting particles via signatures of scattering in the detector target. The first phase aims at operating the detector throughout LHC Run 3 to collect a total of 250 fb^{-1} . This paper provides an overview of the experiment and its aims and reports on the results from the data taken in the first year of its operation, namely the measurement of the muon flux at TI18 and the observation of muon neutrino interactions.

Keywords: neutrino, CERN, LHC, SND@LHC, emulsion, scintillating fibres

DOI: 10.3103/S0027134924701789

1. INTRODUCTION

The neutrino physics program at the LHC started in the 1980s [1–3] with the original suggestions to use a detector to register neutrinos from an LHC-produced flux in a very high pseudorapidity range ($\eta > 7$). Proton–proton (pp) collisions at the LHC produce intense high-energy (10^2 – 10^3 GeV) neutrino fluxes in the forward region, which allows us to explore this yet-barely-probed energy domain [4]. A small-scale LHC experiment can register neutrinos of all three types allowing for the use of the neutrino fluxes created as a side product of primarily charm decays from pp collisions without substantial additional costs.

SND@LHC (Scattering and Neutrino Detector at the LHC [5]) is a compact standalone experiment, which was designed exactly for such a purpose. Located off axis in TI18, a former transfer line from SPS

to LEP, 480 m downstream of the ATLAS interaction point (IP1) [6], it is shielded by approximately 100 m of rock, concrete and LHC magnets deflecting the charged particles from the pp beams. It is capable of identifying neutrinos of all three types in the $7.2 < \eta < 8.4$ pseudorapidity range with high accuracy.

The detector was installed in TI18 in 2021 during the Long Shutdown 2 and started to collect data since the beginning of the LHC Run 3 in April 2022. During the 2022 run it has accumulated a total luminosity of 36.8 fb^{-1} with detector operation uptime $\sim 95\%$. Additional 30 fb^{-1} were collected in 2023.

In this work, we report the detection of ν_μ charged current interactions using the data that was taken by the electronic detectors of the SND@LHC experiment in 2022.

2. SCIENTIFIC PROGRAM

Neutrino measurements are both a way of further testing the Standard Model [7–12] and a great probe

*E-mail: nanti93@mail.ru

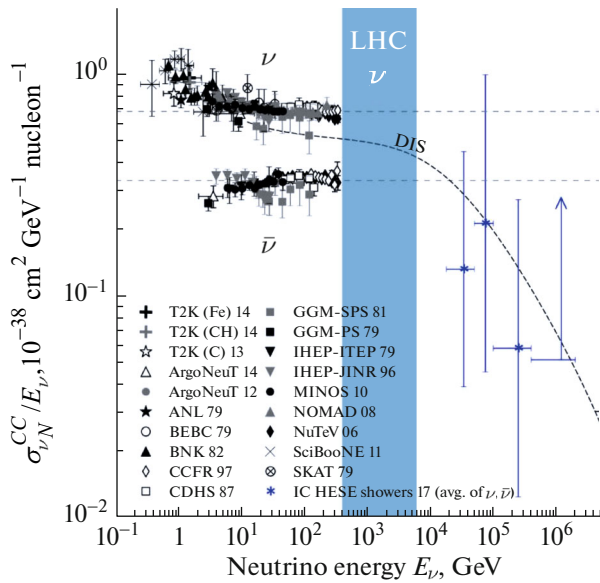


Fig. 1. Overview of the neutrino cross-section measurement at different energies [4].

into the New Physics [13, 14]. The main goals of the experiment can be divided into four categories: (i) neutrino interactions, (ii) heavy flavor physics, (iii) flavor universality tests, and (iv) new physics.

(i) Figure 1 shows the current measurements of neutrino cross sections. As it can be seen from the plot, the region between 350 GeV and 10 TeV is completely unexplored, which provides SND@LHC with an opportunity to measure neutrino cross sections in that region. A measurement of the ratio between charged current (CC) and neutral current (NC) interactions can also serve as an internal consistency check.

(ii) 90% of ν_e and most of ν_τ reaching the SND@LHC come from charmed hadron decays. This provides opportunities to measure the $pp \rightarrow \nu_X$ cross section and forward charm production with neutrinos, as well as to constrain the gluon particle distribution function at very small values of x .

(iii) Detection of all three types of neutrinos allows for tests of lepton flavor universality using two specific ratios of events: ν_e/ν_μ and ν_e/ν_τ .

(iv) SND@LHC provides a way to explore the Hidden Sector through direct model-independent search for feebly interacting particles (FIPs) that decay in the detector or scatter off the target using recoils and time-of-flight technique.

3. DETECTOR CONSTRUCTION

The hybrid detector design of SND@LHC is optimized for the identification of three neutrino flavors and feebly interacting particles and consists of three

parts (see Fig. 2): the veto system, the target section and the hadronic calorimeter (HCAL) with muon identification system.

The veto system is located upstream of the target region and consists of two parallel planes of stacked scintillating bars with readout SiPMs on both ends. This system is used to tag muons and other charged particles entering the detector from the IPI direction.

The target section contains five walls (~ 830 kg) of target tungsten plates interleaved with nuclear emulsion cloud chamber (ECC) plates [16] and followed by stations of electronic trackers made of scintillating fibers (SciFi) [17]. The submicrometric spatial resolution of the nuclear emulsions allows for very efficient tracking of all the charged particles produced in high-energy neutrino interactions, as well as the tau lepton and its decay vertex. Nuclear emulsion films are read out by state-of-the-art, fully automated, optical scanning systems [18–21]. The electronic tracker is used for calorimetry and also provides a timestamp for the recorded events. The single particle spatial resolution is of the order of $\sim 150 \mu\text{m}$ and the time resolution for a particle crossing a station is ~ 250 ps.

The muon system and hadronic calorimeter consist of two parts: upstream (US), the first five stations, and downstream (DS), the last three stations. The stations are made of plastic scintillator plates and interleaved with 20 cm-thick iron walls. The US stations are comprised of 10 horizontal scintillator bars, while the DS stations are made of two layers of finer bars placed perpendicularly to each other allowing for better muon tracking with a spatial resolution less than 1 cm. Every scintillating bar is read out by SiPMs. The muon system can be used in combination with SciFi, reaching $\sim 9.5\lambda_{\text{int}}$ interaction lengths in total and thus providing the energy measurement of hadronic jets.

4. PHYSICS RESULTS

After its successful launch in April 2022, SND@LHC has produced two main results to date: a muon flux measurement and the detection of eight charged current muon neutrino events using the full 2022 run dataset (36.8 fb^{-1}).

The muon flux measurement was done independently for the SciFi and the DS stations and cross-checked with Monte Carlo simulations with the analyzed data samples taken during the 2022 LHC proton run. The measured muon flux using the SciFi amounted to $2.06 \pm 0.01(\text{stat}) \pm 0.11(\text{sys}) \times 10^4 \text{ fb/cm}^2$, while for the DS it counted $2.35 \pm 0.01(\text{stat}) \pm 0.08(\text{sys}) \times 10^4 \text{ fb/cm}^2$ [22]. The resulting agreement between data and Monte Carlo simulations is at the level of 20–25%. The difference

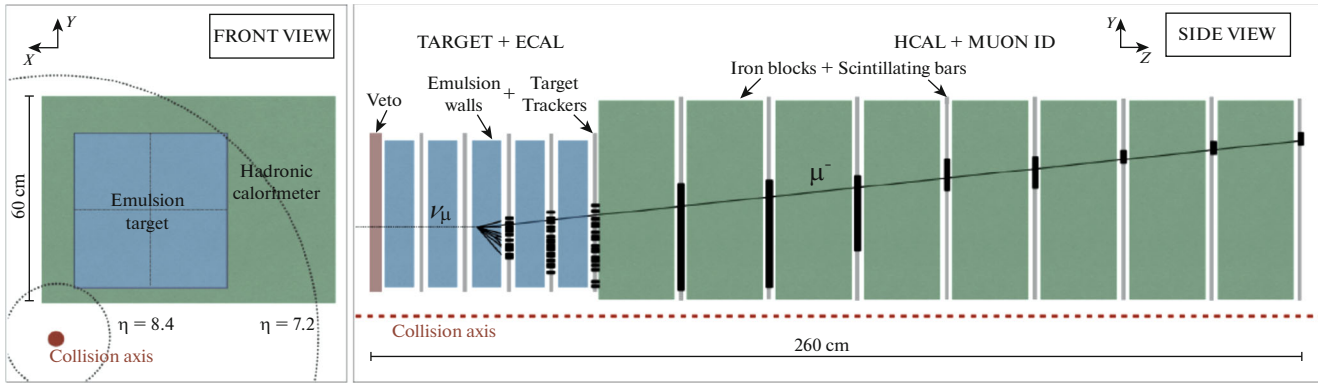


Fig. 2. Schematic layout of the SND@LHC detector front view (left) and side view (right) [15]. The side view includes an illustration of a ν_μ CC event with a visible muon track and a hadronic shower registered by several detectors.

between the estimates is due to a vertical gradient of the flux and the different areas of acceptance of SciFi and DS.

The next study done by SND@LHC aimed to obtain a high-purity sample of CC deep inelastic scattering (DIS) muon neutrino events. The detection of muon neutrino events presupposed an analysis strategy with high rejection power due to the background signal dominating over the neutrino signal. The event selection was based on a fiducial volume cut and a muon identification cut. The fiducial volume cut rejected side-entering backgrounds and any events with a neutral vertex outside the 3rd and the 4th target walls (1st and 2nd wall are rejected to reduce muon-

induced backgrounds and 5th wall is rejected so that neutrino-induced hadronic showers are registered by at least two SciFi stations). The muon identification cut selected the events that a) have large hadronic activity in SciFi and HCAL and b) have a reconstructed and isolated muon track. After the application of all of these cuts, the total number of CC events expected in the whole dataset was 4.2.

There are two main sources of background to the muon neutrino signal: muons entering the fiducial volume without being vetoed (they generate showers via bremsstrahlung or DIS) and neutral particles, mainly neutrons and K_L^0 's, produced in DIS muon interactions in the concrete and rock upstream to the detector (they can mimic the neutrino signal when interacting within the detector). With the total number of muons on acceptance for the considered dataset $N_\mu \sim 5 \times 10^8$ muons [22], the combined inefficiency of the muon system and the first two SciFi stations was estimated as 5.3×10^{-12} , which makes the muon-induced background completely negligible. As for the neutral hadron background, its yield after applying the selection criteria was estimated using the Geant4 toolkit [23] and amounted to $8.6 \pm 3.8 \times 10^{-2}$ events.

With the background-only hypothesis assumed as a null hypothesis, in [15] the Collaboration has reported the observation of 8 candidate events consistent with ν_μ CC interactions with a statistical significance of 6.8 standard deviations (see Fig. 3). Figure 4 shows one of the selected candidate events.

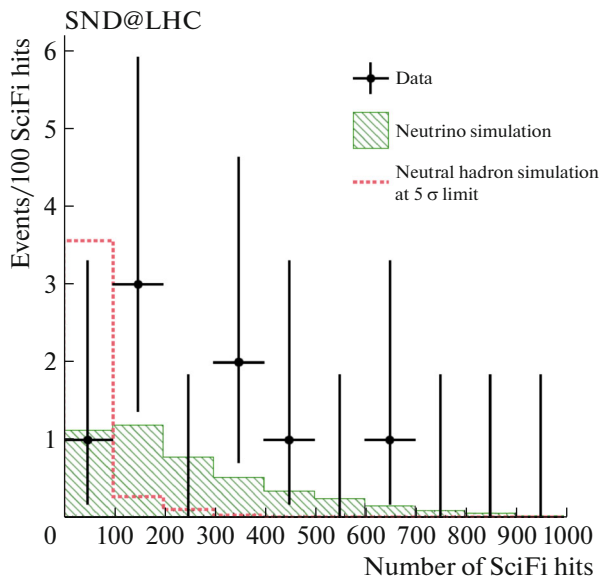


Fig. 3. Distribution of SciFi hits for candidate events, along with the expectation from the neutrino signal [15]. The dashed line shows the background-only hypothesis scaled up to a deviation from the nominal expectation at a level of 5 standard deviations.

FUNDING

This work was supported by ongoing institutional funding. No additional grants to carry out or direct this particular research were obtained.

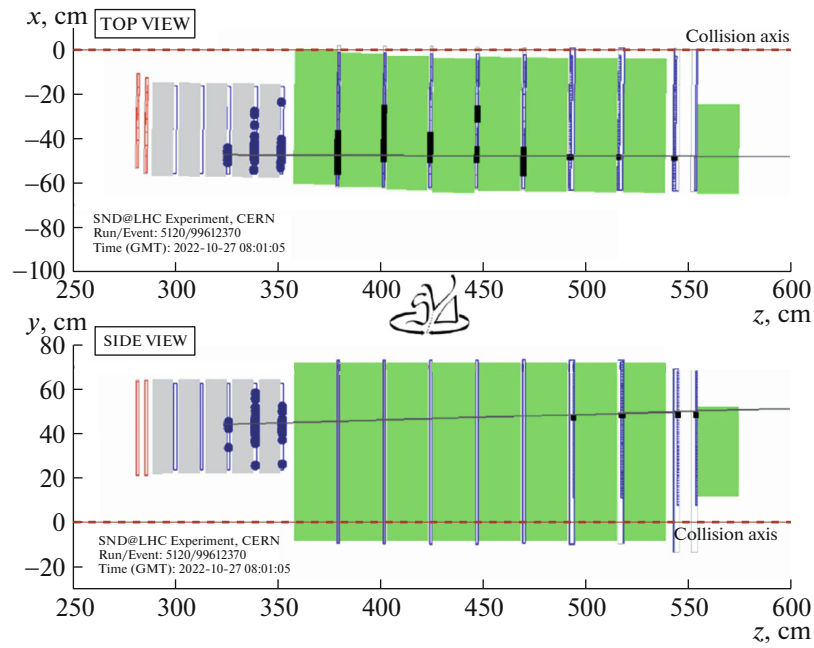


Fig. 4. Display of a ν_μ CC candidate event [15].

CONFLICT OF INTEREST

The authors declare that they have no conflicts of interest.

REFERENCES

1. A. De Rújula and R. Rückl, in *Proc. SSC Workshop: Superconducting Super Collider Fixed Target Physics* (1984), p. 571.
<https://doi.org/10.5170/CERN-1984-010-V-2.571>
2. A. De Rújula, E. Fernández, and J. J. Gómez-Cadenas, *Nucl. Phys. B* **405**, 80 (1993).
[https://doi.org/10.1016/0550-3213\(93\)90427-q](https://doi.org/10.1016/0550-3213(93)90427-q)
3. F. Vannucci, Technical Report No. LPNHE-93-03 (University of Paris, Paris, 1993).
<https://cds.cern.ch/record/253670>.
4. M. Bustamante and A. Connolly, *Phys. Rev. Lett.* **122**, 41101 (2019).
<https://doi.org/10.1103/physrevlett.122.041101>
5. SND@LHC Collab., arXiv Preprint (2023).
<https://doi.org/10.48550/arXiv.2210.02784>
6. ATLAS Collab., *Eur. Phys. J. C* **76**, 653 (2016).
<https://doi.org/10.1140/epjc/s10052-016-4466-1>
7. G. Stermann, J. Smith, J. C. Collins, J. Whitmore, R. Brock, J. Huston, J. Pumplin, W.-K. Tung, H. Weerts, C.-P. Yuan, S. Kuhlmann, S. Mishra, J. G. Morfin, F. Olness, J. Owens, J. Qiu, and D. E. Soper, *Rev. Mod. Phys.* **67**, 157 (1995).
<https://doi.org/10.1103/RevModPhys.67.157>
8. J. M. Conrad, M. H. Shaevitz, and T. Bolton, *Rev. Mod. Phys.* **70**, 1341 (1998).
<https://doi.org/10.1103/revmodphys.70.1341>
9. J. A. Formaggio and G. P. Zeller, *Rev. Mod. Phys.* **84**, 1307 (2012).
<https://doi.org/10.1103/revmodphys.84.1307>
10. G. De Lellis, P. Migliozi, and P. Santorelli, *Phys. Rep.* **399**, 227 (2004).
<https://doi.org/10.1016/j.physrep.2004.07.005>
11. S. Alekhin, W. Altmannshofer, T. Asaka, B. Batell, F. Bezrukov, K. Bondarenko, A. Boyarsky, K.-Y. Choi, C. Corral, N. Craig, D. Curtin, S. Davidson, A. De Gouvêa, S. DelOro, P. Deniverville, P. S. Bhupal Dev, H. Dreiner, M. Drewes, Sh. Ejima, R. Essig, et al., *Rep. Prog. Phys.* **79**, 124201 (2016).
<https://doi.org/10.1088/0034-4885/79/12/124201>
12. H. Abreu, C. Antel, A. Ariga, T. Ariga, J. Boyd, F. Cadoux, D. W. Casper, X. Chen, A. Coccaro, C. Dozen, P. B. Denton, Ya. Favre, J. L. Feng, D. Ferrere, I. Galon, S. Gibson, S. Gonzalez-Sevilla, S.-C. Hsu, Zh. Hu, G. Iacobucci, S. Jakobsen, R. Jansky, E. Kajomovitz, F. Kling, S. Kuehn, L. Levinson, et al. (FASER Collab.), *Eur. Phys. J. C* **80**, 61 (2020).
<https://doi.org/10.1140/epjc/s10052-020-7631-5>
13. D. Marfatia, D. W. McKay, and T. J. Weiler, *Phys. Lett. B* **748**, 113 (2015).
<https://doi.org/10.1016/j.physletb.2015.07.002>
14. C. A. Argüelles, A. J. Aurisano, B. Batell, J. Berger, M. Bishai, T. Boschi, N. Byrnes, A. Chatterjee, A. Chodos, T. Coan, Y. Cui, A. De Gouvêa, P. B. Denton, A. De Roeck, W. Flanagan, D. V. Forero, R. P. Gandrajula, A. Hatzikoutelis, M. Hostert, B. Jones, B. J. Kayser, K. J. Kelly, D. Kim, J. Kopp, A. Kubik, K. Lang, I. Lepetic, P. A. N. Machado, C. A. Moura, F. Olness, J. C. Park, S. Pascoli, S. Prakash, L. Rogers, I. Safa, A. Schneider, K. Scholberg, S. Shin, I. M. Shoemaker,

- G. Sinev, B. Smithers, A. Sousa, Y. Sui, V. Takhistov, J. Thomas, J. Todd, Y.-D. Tsai, Y.-T. Tsai, J. Yu, and C. Zhang, *Rep. Prog. Phys.* **83**, 124201 (2020).
<https://doi.org/10.1088/1361-6633/ab9d12>
15. R. Albanese, A. Alexandrov, F. Alicante, A. Anokhina, T. Asada, C. Battilana, A. Bay, C. Betancourt, R. Biswas, A. Blanco Castro, M. Bogomilov, D. Bonacorsi, W. M. Bonivento, P. Bordalo, A. Boyarsky, S. Buontempo, M. Campanelli, T. Camporesi, V. Canale, A. Castro, D. Centanni, F. Cerutti, M. Chernyavskiy, K.-Y. Choi, et al. (The SND@LHC Collab.), *Phys. Rev. Lett.* **131**, 31802 (2023).
<https://doi.org/10.1103/physrevlett.131.031802>
 16. A. Ariga, T. Ariga, G. De Lellis, A. Ereditato, and K. Niwa, in *Particle Physics Reference Library* (Springer, New York, 2020), Vol. 2, p. 383.
https://doi.org/10.1007/978-3-030-35318-6_9
 17. LHCb Collab., Tech. Rep. 1647400 (CERN, Geneva, 2014). <https://cds.cern.ch/record/1647400>.
 18. A. Alexandrov, A. Buonauro, L. Consiglio, N. D'Ambrosio, G. D. Lellis, A. Di Crescenzo, N. Di Marco, G. Galati, A. Lauria, M. C. Montesi, F. Pupilli, T. Shchedrina, V. Tioukov, and M. Vladymyrov, *J. Instrum.* **10**, P11006 (2015).
<https://doi.org/10.1088/1748-0221/10/11/p11006>
 19. A. Alexandrov, A. Buonauro, L. Consiglio, N. D'Ambrosio, G. De Lellis, A. Di Crescenzo, G. Galati, A. Lauria, M. C. Montesi, V. Tioukov, and M. Vladymyrov, *J. Instrum.* **11**, P06002 (2016).
<https://doi.org/10.1088/1748-0221/11/06/p06002>
 20. A. Alexandrov, A. Buonauro, L. Consiglio, N. D'Ambrosio, G. De Lellis, A. Di Crescenzo, G. Galati, V. Gentile, A. Lauria, M. C. Montesi, V. Tioukov, M. Vladymyrov, and E. Voevodina, *Sci. Rep.* **7**, 7310 (2017).
<https://doi.org/10.1038/s41598-017-07869-3>
 21. A. Alexandrov, G. De Lellis, and V. Tioukov, *Sci. Rep.* **9**, 2870 (2019).
<https://doi.org/10.1038/s41598-019-39415-8>
 22. SND@LHC Collab., arXiv Preprint (2023).
<https://doi.org/10.48550/arXiv.2310.05536>
 23. S. Agostinelli, J. Allison, K. Amako, J. Apostolakis, H. Araujo, P. Arce, M. Asai, D. Axen, S. Banerjee, G. Barrand, F. Behner, L. Bellagamba, J. Boudreau, L. Broglia, A. Brunengo, H. Burkhardt, S. Chauvie, J. Chuma, R. Chytrcek, G. Cooperman, G. Cosmo, P. Degtyarenko, A. Dell'Acqua, G. Depaola, D. Dietrich, R. Enami, A. Feliciello, C. Ferguson, H. Fesefeldt, G. Folger, et al. (GEANT4 Collab.), *Nucl. Instrum. Methods Phys. Res., Sect. A* **506**, 250 (2003).
[https://doi.org/10.1016/s0168-9002\(03\)01368-8](https://doi.org/10.1016/s0168-9002(03)01368-8)

Publisher's Note. Allerton Press, Inc. remains neutral with regard to jurisdictional claims in published maps and institutional affiliations.

AI tools may have been used in the translation or editing of this article.